Algorithms for the Evolution of Electronic Properties in Nanocrystals

James R. Chelikowsky [a,*], Murilo L. Tiago [a], Yousef Saad [c], Yunkai Zhou [d]

[a] *Center for Computational Materials, Institute for Computational Engineering and Science, University of Texas, Austin, TX 78712 USA*

[b] *Departments of Physics and Chemical Engineering, University of Texas, Austin, TX 78712 USA*

[c] *Department of Computer Science and Engineering, University of Minnesota, Minneapolis, MN, 55455 USA*

[d] *Department of Mathematics, Southern Methodist University, Dallas, TX 75275 USA*

Abstract

We illustrate recent progress in developing algorithms for solving the Kohn-Sham problem. Key ingredients of our algorithm include pseudopotentials implemented on a real space grid and the use of damped-Chebyshev polynomial filtered subspace iteration. This procedure allows one to predict electronic properties for many materials across the nano-regime, *i.e.*, from atoms to nanocrystals of sufficient size to replicate bulk properties. We will illustrate this method for large silicon quantum dots.

Key words: Pseudopotentials, nanocrystals, density functional theory, silicon quantum dots

1. Introduction

One of the most significant goals in computational physics is the development of new algorithms and physical concepts for describing matter at all length scales, especially at the nano-scale. This goal has assumed more significance in past years owing to interest in the role of quantum confinement [1]. Quantum confinement offers one the opportunity to alter physical properties of matter without changing the chemical composition. For example, quantum confinement in CdSe nanocrystals can be use to tune the optical gap across the visible spectrum [2] or Si nanocrystals can be made optically active at small length scales [3].

Achieving an efficacious algorithm for predicting the role of quantum confinement and its role in determining the properties of nanocrystals is a difficult task owing to the complexity of nanocrystals, which often contain thousands of atoms. However, notable progress has been accomplished by implementing new algorithms designed for highly parallel platforms. Here we will outline the nature of these algorithms and apply them to complex systems such as large quantum dots.

2. The Electronic Structure Problem

The spatial and energetic distributions of electrons can be described by a solution of the Kohn-Sham equation [4]:

$$\left(\frac{-\hbar^2\nabla^2}{2m} + V_{ion}^p + V_H + V_{xc} \right) \psi_n = E_n \psi_n \quad (1)$$

where V_{ion}^p is an ionic pseudopotential [5], V_H is the Hartree or Coulomb potential, and V_{xc} is the exchange correlation potential. The Hartree and exchange-correlation potentials can be determined from the electronic charge density. The density is given by

* Corresponding author.

Email address: jrc@ices.utexas.edu (James R. Chelikowsky).

$$\rho(\boldsymbol{r}) = e \sum_{n,occup} |\psi_n(\boldsymbol{r})|^2 \tag{2}$$

The summation is over all occupied states. The Hartree potential is then determined by

$$\nabla^2 V_H(\boldsymbol{r}) = -4\pi e \rho(\boldsymbol{r}) \tag{3}$$

This term can be interpreted as the electrostatic interaction of an electron with the charge density of the system.

The exchange-correlation potential is more problematic. This potential can evaluated using a *local density approximation*. The central tenant of this approximation is that the total exchange-correlation energy may be written as a universal functional of the density:

$$E_{xc}[\rho] = \int \rho(\boldsymbol{r})\ \epsilon_{xc}[\rho(\boldsymbol{r})]\ d^3r \tag{4}$$

where ϵ_{xc} is the exchange-correlation energy density. E_{xc} and ϵ_{xc} are to be interpreted as depending solely on the charge density. The exchange-correlation potential, V_{xc}, is then obtained as $V_{xc} = \delta E_{xc}[\rho]/\delta\rho$.

It is not difficult to solve the Kohn-Sham equation (Eq. 1) for an atom. The atomic charge density can be taken to be spherically symmetric. Thus, the Kohn-Sham problem reduces to solving a one-dimensional problem. The Hartree and exchange-correlation potentials can be iterated to form a self-consistent field. This atomic solution provides the input to construct a pseudopotential representing the effect of the core electrons and nucleus. This "ion core" pseudopotential, V^p_{ion}, can be transferred to other systems such as molecules and quantum dots [5].

The Kohn-Sham equations represent a nonlinear, self-consistent eigenvalue problem. Typically, a solution is obtained by first approximating the Hartree and exchange-correlation potentials using a superposition of atomic charge densities. The Kohn-Sham equation is then solved using these approximate potentials. From the solution, new wave functions and charge densities are obtained and used to construct updated Hartree and exchange-correlation potentials. The process is repeated until the "input" and "output" potentials agree and a self-consistent solution is realized. At this point, the total electronic energy can be computed along with a variety of other electronic properties [5].

Once the Kohn-Sham equation is solved, the total electronic energy, E_T, of the system can be evaluated from

$$\begin{aligned} E_T = &\sum_{n,occup} E_n - \frac{1}{2}\int V_H(\boldsymbol{r})\rho(\boldsymbol{r})\ d^3r \\ &+ \int \rho(\boldsymbol{r})\ (\epsilon_{xc}[\rho(\boldsymbol{r})] - V_{xc}[\rho(\boldsymbol{r})])\ d^3r \end{aligned} \tag{5}$$

The structure energy can be obtained by adding the ion core electrostatic terms [5]. The forces can be obtained by taking the derivative of the energy with respect to position.

3. Algorithms for Solving the Kohn-Sham Equation

The Kohn-Sham equation as cast in Eq. 1 can be solved using a variety of techniques. Often the wave functions can be expanded in a basis such as plane waves or gaussians and the resulting secular equations can be solved using standard diagonalization packages such as those found in VASP [6].

Here we focus on a different approach. We solve the Kohn-Sham equation without resort to an explicit basis [7–10]. We solve for the wave functions on the grid with a fixed domain, which encompasses the physical system of interest. The grid need not be uniform, but it greatly simplifies the problem if it is. The wave functions outside of the domain are required to vanish for confined systems or assume periodic boundary conditions for systems with translational symmetry. In contrast to methods employing an explicit basis, such boundary conditions are easily incorporated. In particular, real space methods do not require the use of supercells for localized systems. As such, charged systems can easily be examined without considering any electrostatic divergences.

Within a "real space" approach, one can solve the eigenvalue problem using a finite element or finite difference approach [8,10]. We use a higher order finite difference approach owing to its simplicity in implementation. The Laplacian operator can be expressed using

$$\left(\frac{\partial^2\psi}{\partial x^2}\right)_{x_0} \approx \sum_{n=-N}^{N} C_i\ \psi(x_0 + nh, y, z) \tag{6}$$

where h is the grid spacing, N is the number of nearest grid points, and C_i are the coefficients for evaluating the required derivatives [11]. The error scales as $O(h^{2N+2})$.

Once the secular equation is created, the eigenvalue problem can be solved using iterative methods [9,12]. Typically, a method such as a preconditioned Davidson method can be used. This is a

robust and efficient method, which never requires one to store the Hamiltonian matrix. In this paper we outline a method that avoids solving large eigenvalue problems explicitly [9]. The method utilizes a damped *Chebyshev polynomial filtered subspace iteration*. In our approach, only the initial iteration requires solving an eigenvalue problem, which can be handled by means of any available efficient eigensolver. This step is used to provide a good initial subspace (or good initial approximation to the wave functions). Because the subspace dimension is slightly larger than the number of wanted eigenvalues, the method does not require as much memory as standard restarted eigensolvers such as ARPACK and TRLan (Thick - Restart, Lanczos) [13,14]. Moreover, the cost of orthogonalization is much reduced as the filtering approach only requires a subspace with dimension slightly larger than the number of occupied states and orthogonalization is performed only once per SCF iteration. In contrast, standard eigensolvers using restart usually require a subspace twice as large and the orthogonalization and other costs related to updating the eigenvectors are much higher.

The main idea of the proposed method is to start with a good initial eigen-basis, $\{\psi_n\}$, corresponding to occupied states of the initial Hamiltonian, and then to improve adaptively the subspace by polynomial filtering. That is, at a given self-consistent step, a polynomial filter, $P_m(t)$, of order m is constructed for the current Hamiltonian $\mathcal{H}$. As the eigen-basis is updated, the polynomial will be different at each SCF step since $\mathcal{H}$ will change. The goal of the filter is to make the subspace spanned by $\{\hat{\psi_n}\} = P_m(\mathcal{H})\{\psi_n\}$ approximate the eigen subspace corresponding to the occupied states of $\mathcal{H}$. There is no need to make the new subspace, $\{\hat{\psi_n}\}$, approximate the wanted eigen subspace of $\mathcal{H}$ to high accuracy at intermediate steps. Instead, the filtering is designed so that the new subspace obtained at each self-consistent iteration step will progressively approximate the wanted eigen space of the final Hamiltonian when self-consistency is reached.

This can be efficiently achieved by exploiting the Chebyshev polynomials, C_m, for the polynomials: P_m. Specifically, we wish to exploit the fast growth property outside of the [-1, 1] interval. All that is required to obtain a good filter at a given SCF step, is to provide a lower bound and an upper bound of an interval of the spectrum of the current Hamiltonian $\mathcal{H}$. The lower bound can be readily obtained from the Ritz values computed from the previous step, and the upper bound can be inexpensively obtained by a very small number of (*e.g.*, 4 or 5) Lanczos steps [9]. Hence the main cost of the filtering at each iteration is in computing the polynomial operation.

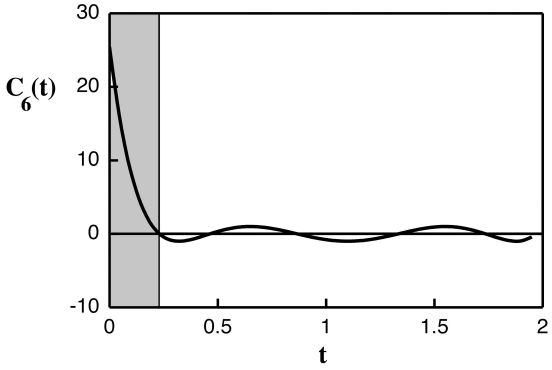

Fig. 1. Example of a damped Chebyshev polynomial, C_6, the shaded area corresponds to eigenvalue spectrum regime that will be enhanced by the filtering operation (see text).

To construct a "damped" Chebyshev polynomial on the interval [a,b] to the interval [-1,1], one can use an affine mapping such that

$$l(t) = \frac{t - (a+b)/2}{(b-a)/2} \tag{7}$$

The interval is chosen to encompass the energy interval containing the eigen space of interest, *i.e.*, the lowest to highest eigenvalues. The filtering operation can then be expressed as

$$\{\hat{\psi_n}\} = C_m(l(\mathcal{H}))\{\psi_n\} \tag{8}$$

This computation is accomplished by exploiting the convenient three-term recurrence property of Chebyshev polynomials:

$$\begin{aligned} C_0(t) = 1 \qquad C_1(t) = t \\ C_{m+1}(t) \;=\; 2t\; C_m(t) \;-\; C_{m-1}(t) \end{aligned} \tag{9}$$

An example of a damped Chebyshev polynomial as defined by Eqs. 7 and 9 is given in Fig. 1 where we have taken the lower bound as a=0 and the upper bound as b=2. In this example, the filtering would enhance the eigenvalue components in the shaded region.

The filtering procedure for the self-consistent cycle is illustrated in Fig. 2. Unlike traditional methods, the cycle only requires one explicit diagonalization step. Instead of repeating this step again within the self-consistent loop, a filtering operation is used to create a new basis in which the desired eigen subspace is enhanced. After the new basis, $\{\hat{\psi_n}\}$,

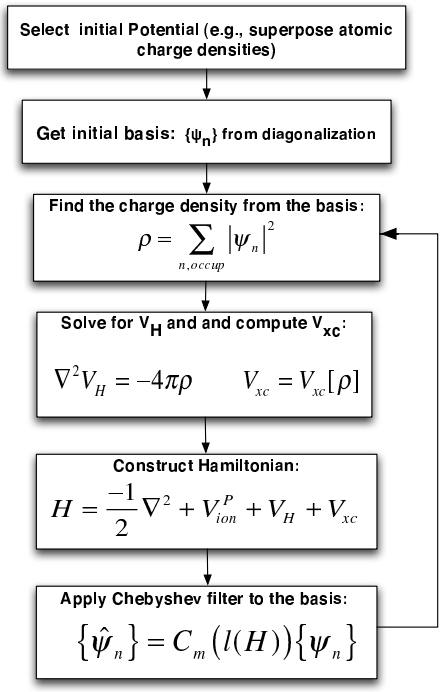

Fig. 2. Schematic of the self-consistent cycle using Chebyshev filtering.

is formed, the basis is orthogonalized. The orthogonalization step scales as the cube of the number of occupied states and as such this method is not an "order-n" method. However, the prefactor is sufficiently small that the method is much faster than previous implementations of real space methods [9]. The cycle is repeated until the "input" and "output" density is unchanged.

In Table 1, we compare the timings using the Chebyshev filtering method along with explicit diagonalization solvers using the TRLan and the ARPACK. These timing are for a modest sized quantum dot: $Si_{525}H_{276}$. The Hamiltonian size is 292,584 × 292,584 and 1194 eigenvalues were determined. The numerical runs were performed on the SGI Altix 3700 cluster at the Minnesota Supercomputing Institute. The CPU type is a 1.3 GHz Intel Madison processor. Although the number of matrix-vector products and SCF iterations is similar, the total time with filtering is over an order of magnitude faster compared to ARPACK and a factor of better than four versus the TRALan. Such improved timings are not limited to this particular example. We have also explored GaAs quantum dots and large Fe clusters, including spin-dependent density functionals.

Method	H×	SCF Its	CPU(s)
Filtering	124,761	11	5,946.7
ARPACK	142,047	10	62,026.4
TRLan	145,909	10	26,852.8

Table 1. Comparison of the Chebyshev flitering method compared to one based on ARPACK. $H\times$ indicates the number of matrix-vector products, $SCFIts$ indicates the number of iterations for a self-consistent solution and the last entry is the CPU time in seconds.

4. Application: Electronic Properties of Silicon Quantum Dots

We will illustrate the Chebyshev filtering method for a nano scale system: hydrogenated silicon quantum dots. We will consider systems that are beyond the computational limits of "standard" methods for obtaining a solution to the Kohn-Sham problem.

Quantum dots are small fragments of the bulk in which the surface has been passivated. In the case of silicon, the passivation is accomplished experimentally by capping the surface dangling bonds with hydrogen atoms [15]. These systems exhibit interesting changes as one approaches the nano-regime. For example, nanocrystals of silicon are expected to be optically active, whereas bulk crystals of silicon are not [15,16].

The largest dot we examined contained over ten thousand atoms: $Si_{9041}H_{1860}$ This dot is approximately 7 nm in diameter. A ball and stick model for such quantum dots is illustrated in Fig. 3.

A solution of the Kohn-Sham Eq. 1 will yield the energy levels or eigenstates for the quantum dot. If the dot is sufficiently large, this spectrum should approach the density of states of crystalline silicon. This is illustrated in Fig. 4. The bulk density of states will reflect van Hove singularities in the energy band topology, *i.e.* , singularities associated with critical points when $\nabla_{\boldsymbol{k}} E(\boldsymbol{k})$ vanishes (where $E(\boldsymbol{k})$ is the energy band as a function of the wave vector [17]). The generally good agreement between the density of states for the dot and crystal suggests that by ∼7 nm the dot is of sufficient size to capture the van Hove singularities. (The compari-

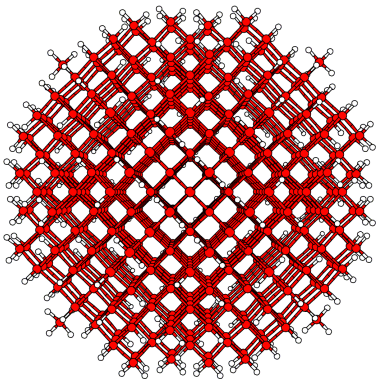

Fig. 3. Ball and stick model of a hydrogenated silicon quantum dot. The interior consists of a diamond fragment. The surface of the fragment is capped with hydrogen atoms.

son will not be exact because the quantum dot contains Si-H bonds in addition to the Si-Si bonds. In the dot eigenvalue spectrum, this results in the extra contributions near 5 eV.)

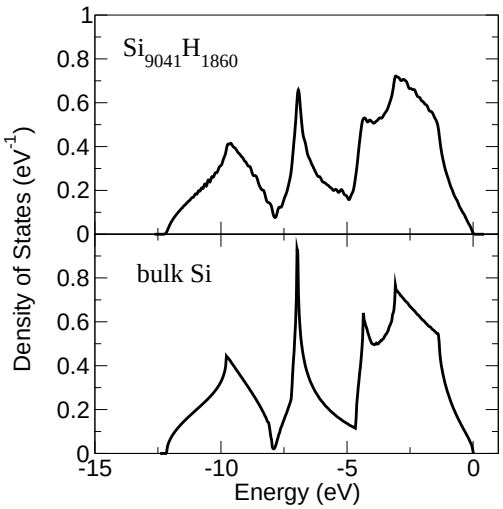

Fig. 4. Eigenvalue spectrum for a large quantum dot of silicon: $Si_{9041}H_{1860}$ (top panel) compared to the density of states of crystalline silicon (bottom panel). The energy zero is taken to the highest occupied level for the dot and the valence band maximum for the crystal.

We can also examine the evolution of the ionization potentials (I) and the electron affinities (A) for the quantum dot:

$$\begin{aligned} I &= E(N-1) - E(N) \\ A &= E(N) - E(N+1) \end{aligned} \tag{10}$$

The difference between the ionization potential and the electron affinity can be associated with the quasi-particle gap: E_{qp}=I-A. If the exciton (electron-hole) interaction is small, this gap can be compared to the optical gap. However, for silicon quantum dots the exciton energy is believe to be on the order of ∼1 eV for dots less than ∼1 nm.

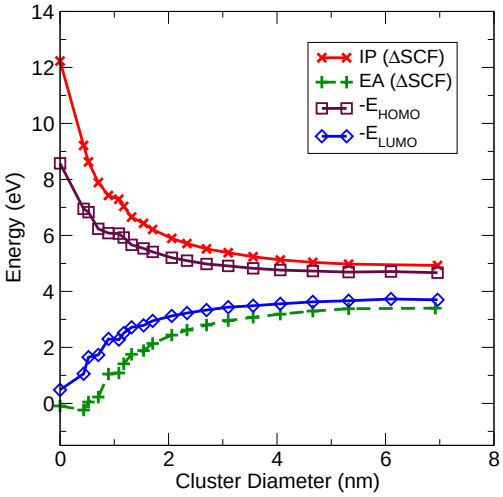

Fig. 5. Evolution of the ionization potential (IP) and electron affinity (EA) with quantum dot size. Also shown are the eigenvalue levels for the high occupied molecular orbital (HOMO) and the lowest unoccupied molecular orbital (LUMO).

We can examine the scaling of the ionization potential and affinity by assuming a simple scaling and fitting to the calculated values (shown in Fig. 5):

$$\begin{aligned} I(D) &= I_\infty + A/D^\alpha \\ A(D) &= A_\infty + B/D^\beta \end{aligned} \tag{11}$$

where D is the dot diameter. A fit of these quantities results in I_∞=4.5 eV, A_∞=3.9 eV, α=1.1 and β=1.08. The fit gives a quasi-particle gap of $E_{qp}(D \to \infty) = I_\infty - A_\infty$=0.6 eV in the limit of an infinitely large dot. This value is good agreement with the gap found for crystalline silicon using the local density approximation [18]. The gap is not in good agreement with experiment owing to the failure of density functional theory to describe excited states.

A key aspect of our study is that we can examine the scaling of the ionization potential and electron affinity for quantum dots ranging from silane (SiH_4) to dots with thousand of atoms. We not only verify the limiting value of the quasi-particle gap, we can

ascertain how this limit is reached, *i.e.*, how the ionization potential and electron affinity scale with the size of the dot and what the relationship is between theses quantities and the highest occupied and lowest empty energy levels.

5. Conclusions

The algorithm presented in this paper replaces the explicit eigenvalue calculations by an approximation of the wanted invariant subspace, obtained with the use of Chebyshev polynomial filters. In our approach, only the initial self-consistent field iteration requires solving an eigenvalue problem in order to provide a good initial subspace. In the remaining iterations, no iterative eigensolvers are involved. Instead, Chebyshev polynomials are used to refine the subspace. The subspace iteration at each step is easily five to ten times faster than solving a corresponding eigenproblem by the most efficient eigen-algorithms. Moreover, the subspace iteration reaches self-consistency within roughly the same number of steps as an eigensolver-based approach. This results in a significantly faster SCF iteration.

We illustrated this algorithm by applying it to hydrogenated silicon quantum dots. The largest dot we examined contained over 10,000 atoms and was ~ 7 nm ($Si_{9041}H_{1860}$) in diameter. We examined the evolution of the electronic properties in these dots by examining the density of states, which we found to assume a bulk-like configuration for dots larger than ~ 5 nm. In addition, we obtained scaling relations for the ionization potential, the electron affinity and the quasi-particle gap over the size regime of interest. We found the quasi-particle gap to approach the known bulk limit within density functional theory.

Acknowledgements

This work was supported in part by the National Science Foundation under DMR-0551195 and the US Department of Energy under DE-FG02-89ER45391 and DE-FG02-03ER15491. Calculations were performed at the Texas Advanced Computing Center (TACC), Minnesota Supercomputing Institute (MSI) and National Energy Research Scientific Computing Center (NERSC).

References

[1] A. P. Alivisatos, Science 271 (1996) 933.

[2] C. Troparevsky and L. Kronik and J. R. Chelikowsky, J. Chem. Phys. 119 (2003) 2284.

[3] I. Vasiliev, J. R. Chelikowsky, and R. M. Martin, Phys. Rev. B 65 (2002) 121302 and I. Vasiliev, S. Ogut and J. R. Chelikowsky, Phys. Rev. B 65 (2002) 115416.

[4] W. Kohn and L. J. Sham, Phys. Rev. 140 (1965) A1133.

[5] J. R. Chelikowsky and M. L. Cohen, "Pseudopotentials for Semiconductors" in Handbook of Semiconductors, edited by T. S. Moss and P. T. Landsberg, Volume 1, Elsevier, Amsterdam, 1992, p. 59; J. R. Chelikowsky, J. Phys. D 33 (2000) R33.

[6] G. Kresse and J. Furthmüller, Phys. Rev. B 54 (1996) 11169 and http://cms.mpi.univie.ac.at/vasp/.

[7] J. R. Chelikowsky, N. Troullier, and Y. Saad, Phys. Rev. Lett. 72 (1994) 1240. Also, see http://www.ices.utexas.edu/parsec/.

[8] T. Torsti, T. Eirola, J. Enkovaara, T. Hakala, P. Havu, V. Havu, T. Höynälänmaa, J. Ignatius, M. Lyly, I. Makkonen, T. T. Rantala, J. Ruokolainen, K. Ruotsalainen, E. Räsänen, H. Saarikoski, and M. J. Puska, phys. stat. solidi (b) 243 (2006) 1016; L. Kronik, A. Makmal, M.L. Tiago, M.M.G. Alemany, M. Jain, X. Huang, Y. Saad and J.R. Chelikowsky, phys. stat. sol. (b) 243 (2006) 1063 and references therein.

[9] Y. Zhou, Y. Saad, M. L. Tiago and J. R. Chelikowsky, Journal of Computational Physics, (2006) in press.

[10] T. L. Beck, Rev. Mod. Phys. 74 (2000) 1041.

[11] B. Fornberg and D. M. Sloan, Acta Numerica 94 (1994) 203.

[12] A. Stathopoulos, S. Öğüt, Y. Saad, J.R. Chelikowsky and H. Kim, IEEE Comput. Sci. Eng. 2 (2000) 19; C. Bekas, Y. Saad, M.L. Tiago and J.R. Chelikowsky, Comp. Phys. Comm. 171 (2005) 175.

[13] R. B. Lehoucq, D. C. Sorensen, and C. Yang. ARPACK Users Guide: Solution of Large Scale Eigenvalue Problems by Implicitly Restarted Arnoldi Methods, SIAM, Philadelphia, 1998. The software is available at http://www.caam.rice.edu/software/ARPAC.

[14] K. Wu, A. Canning, H. D. Simon and L. -W. Wang, J. Comp. Phys. 154 (1999) 156.

[15] S. Furukawa and T. Miyasato, Phys. Rev. B 38 (1988) 5726.

[16] S. Ogut, J. R. Chelikowsky and S. G. Louie, Phys. Rev. Lett. 79 (1997) 1770.

[17] J.R. Chelikowsky and M.L. Cohen, Phys. Rev. B 14 (1976) 556.

[18] L. J. Sham and M. Schlüter, Phys. Rev. Lett. 51 (1983) 1888; J. P. Perdew and M. Levy, Phys. Rev. Lett. 51 (1983) 1884.